*Biodegradation* **10:** 201–217, 1999.

# Intrinsic bioremediation of a petroleum hydrocarbon-contaminated aquifer and assessment of mineralization based on stable carbon isotopes

Christof Bolliger*, Patrick Höhener, Daniel Hunkeler, Katharina Häberli & Josef Zeyer
*Swiss Federal Institute of Technology (ETH), Institute of Terrestrial Ecology, Soil Biology, CH-8952 Schlieren, Switzerland (*author for correspondence, e-mail: bolliger@ito.umnw.ethz.ch)*

Accepted 4 February 1999

*Key words:* ground water, intrinsic bioremediation, natural gradient tracer test, petroleum hydrocarbons, redox processes, stable carbon isotopes

## Abstract

This study presents a stepwise concept to assess the in situ microbial mineralization of petroleum hydrocarbons (PHC) in aquifers. A new graphical method based on stable carbon isotope ratios ($\delta^{13}$C) was developed to verify the origin of dissolved inorganic carbon (DIC). The concept and the isotope method were applied to an aquifer in Studen, Switzerland, in which more than 34,000 liters of heating oil were accidentally released. Chemical analyses of ground water revealed that in this aquifer locally, anaerobic conditions prevailed, and that PHC mineralization was linked to the consumption of oxidants such as $O_2$, $NO_3^-$, and $SO_4^{2-}$ and the production of reduced species such as $Fe^{2+}$, $Mn^{2+}$, $H_2S$ and $CH_4$. However, alkalinity and DIC balances showed a quantitative disagreement in the link between oxidant consumption and DIC production, indicating that chemical data alone may not be a reliable assessment tool. $\delta^{13}$C ratios in DIC have been used before for bioremediation assessment, but results were reported to be negatively influenced by methanogenesis. Using the new graphical method to display $\delta^{13}$C data, it was possible to identify anomalies found in methanogenic monitoring wells. It could be shown that 88% of the DIC produced in the contaminated aquifer originated from microbial PHC mineralization. Thus, the new graphical method to display $\delta^{13}$C ratios appears to be a useful tool for the assessment of microbial hydrocarbon mineralization in a complex environment.

## Introduction

Contamination of soil and ground water by the accidental release of petroleum hydrocarbons (PHC) is a common problem for drinking water supplies (U.S. National Research Council 1993). At petroleum spill sites, PHC usually migrate vertically downward through the unsaturated zone due to the force of gravity and then laterally along the ground water table (Boulding 1995). Capillary forces and ground water table fluctuations result in the vertical smearing of the PHC phase in the vicinity of the ground water table. The zone where PHC are found as a free phase is designated as the source area (ASTM 1995). More soluble PHC components such as monoaromatic hydrocarbons are continuously released from the source area into the ground water, creating a contaminant plume within the aquifer (Bedient et al. 1994). Field evidence suggests that the extension of many plumes reaches a steady-state distribution due to natural attenuation (Eganhouse et al. 1993; Davis et al. 1994; McAllister & Chiang 1994; Borden et al. 1995). Natural attenuation of PHC in soil and ground water may include a number of processes such as biodegradation by naturally-occurring microorganisms (intrinsic bioremediation), sorption, dispersion, advection, dissolution, and volatilization (Rifai et al. 1995). Biodegradation is the only process that leads to a reduction of the total mass of PHC, but to what extent it contributes to natural attenuation is often difficult to quantify.

Ideally, biodegradation results in complete mineralization of PHC, forming only carbon dioxide, water, and biomass. Although aerobic biodegradation is considered to be the most efficient process to mineralize PHC (Atlas & Bartha 1992), the natural rate of $O_2$ supply within the saturated zone is often not sufficient to meet the $O_2$ demand of aerobic microbial respiration. Therefore, PHC contaminated aquifers usually become anoxic (Baedecker et al. 1993; Bennett et al. 1993; Vroblesky & Chapelle 1994; Landmeyer et al. 1996). Various field and laboratory studies have shown that the mineralization of PHC does not rely exclusively on $O_2$ as an oxidant but can also be coupled to the reduction of $NO_3^-$, Mn(IV), Fe(III), $SO_4^{2-}$ and $CO_2$ (for recent reviews see Holliger & Zehnder 1996 and Krumholz et al. 1996).

The validation of intrinsic bioremediation as an effective remediation strategy requires the demonstration of mineralization of the contaminants in situ (Madsen et al. 1991; U.S. National Research Council 1993; Hunkeler 1997). Supporting evidence typically includes the decrease of contaminant concentrations, the formation of carbon dioxide, the consumption of oxidants, the formation of reduced species, and the formation of biomass. More recently, stable carbon isotopes ratios were used to monitor biodegradation of PHC (Van de Velde et al., 1995; Landmeyer et al. 1996; Aggarwal et al. 1997; Conrad et al. 1997). However, a reliable demonstration of mineralization should include several lines of evidence (Madsen et al. 1991; U.S. National Research Council 1993; Hunkeler 1999).

In this paper, we present a detailed concept to assess intrinsic bioremediation at a heating oil-contaminated site (Studen, Switzerland). The concept includes the following steps: 1) a natural gradient tracer experiment is performed to characterize the ground water transport at the site, 2) the ground water chemistry along the plume centerline is examined and the dominant microbial and geochemical processes occurring in the aquifer are identified, 3) DIC and alkalinity changes in the ground water are measured and subsequently compared with calculated values based on stoichiometric considerations, and finally 4) Stable carbon isotope ratios ($\delta^{13}C$) are used to identify the sources of the produced DIC. The balance of the stable carbon isotopes of the DIC is used to discriminate between DIC produced by mineralization and carbonate dissolution, respectively (Carothers & Kharaka 1980; Boutton 1991; Conrad et al. 1997). The results of our study demonstrate that intrinsic bioremediation is a major process in the removal of PHC at this site.

## Field site description

### *Site and remediation history*

In an urban area in Studen, Switzerland, a spill of more than 34,000 liters of heating oil was discovered in 1993 (Figure 1). Preliminary observations (unpublished data) indicated that an indigenous microbial population had developed following the spill, possibly degrading PHC. Due to these results and the fact that there was no immediate threat to drinking water wells downgradient, the cantonal water protection authorities decided to limit engineered remediation efforts to the physical removal of the free PHC phase by pumping and to monitor natural attenuation processes.

Typical of many polluted sites, the Studen site contains inherent obstacles to the establishment of a quantitative assessment of intrinsic bioremediation. Primarily, it is not known exactly how much heating oil was spilled or when the spill occurred. Secondly, the site is located in an urban area, and part of the contaminated zone is inaccessible due to buildings and underground utilities. Finally, most monitoring wells were installed as part of an emergency physical remediation plan. Therefore, both the diameter of the wells and the length and depth of the screened portions vary. In accessible areas, small trenches were excavated down to the ground water table to localize the contamination. Before refilling the trenches with clean soil, 11 wells were installed using prefabricated concrete pipes (0.6 to 0.8 m diameter) which were screened in the lowest meter. These wells are designated S1–S11 (Table 1). Between 1993 and 1996, about 34,000 liters of heating oil were recovered using floating pumps. After June 1996, no further engineered remediation actions were undertaken.

In January 1993 during the emergency assessment and later in May 1996, several monitoring wells were drilled in less accessible areas in order to estimate the size of the source area and of the plume (wells P1–P17 and P20–P28, respectively). The wells were equipped with either PVC piezometer tubes or steel tubes (P12–P17). All tubes were screened in the saturated part of the aquifer. The zone where the wells contained heating oil in free phase in 1993 was assumed to represent the source area (Figure 1 and Table 1). The source area remained stable after 1993. In May 1996, PVC piezometer tubes screened in their lower parts were placed into five of the concrete wells, and the void space was filled with clean gravel and topped with loam. These wells are designated PS (Table 1).

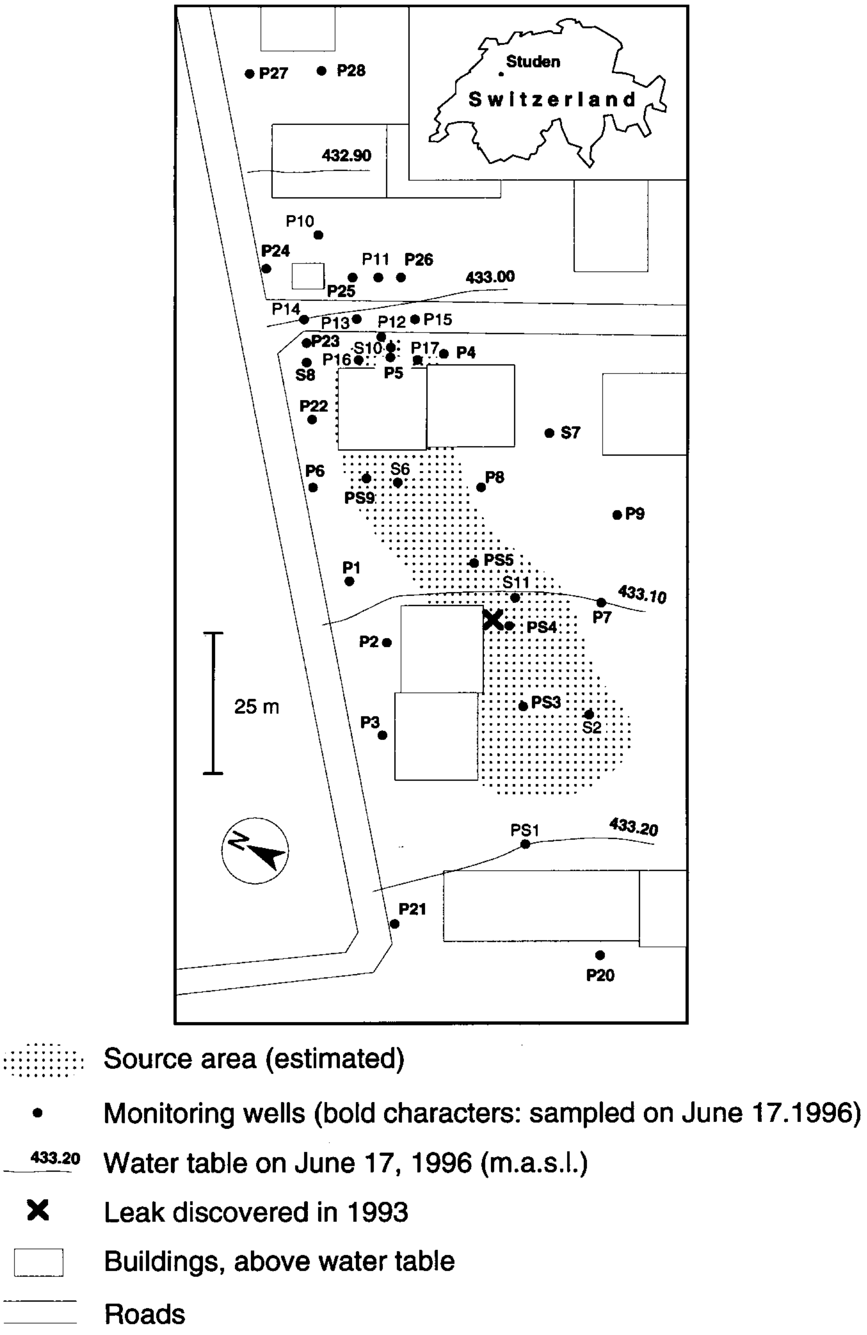

*Figure 1.* Location and map of source area and monitoring wells at the Studen site.

*Table 1.* Overview of all monitoring wells

| Observation well | Diameter cm | Free phase 1993 | Free phase 1996 | Ground water table[a] m.a.s.l.[c] | Bottom of well[b] m.a.s.l.[c] |
|---|---|---|---|---|---|
| S1 → PS1[d] | 60 → 11.5 | – | – | 433.20 | 432.49 |
| S2 | 60 | + | + | 433.16 | 432.63 |
| S3 → PS3[d] | 80 → 11.5 | + | + | 433.16 | 432.65 |
| S4 → PS4[d] | 60 → 11.5 | + | + | 433.14 | 432.45 |
| S5 → PS5[d] | 80 → 11.5 | + | + | 433.09 | 432.69 |
| S6 | 80 | + | + | [e] | 430.93 |
| S7 | 60 | – | – | 433.07 | 432.50 |
| S8 | 60 | – | – | 433.04 | 432.89 |
| S9 → PS9[d] | 80 → 11.5 | + | + | 433.07 | 432.63 |
| S10 | 80 | + | + | [e] | 432.19 |
| S11 | 60 | + | + | 433.11 | 431.63 |
| P1 | 14.5 | – | – | 433.08 | 431.73 |
| P2 | 14.5 | – | – | 433.11 | 431.70 |
| P3 | 14.5 | – | – | 433.16 | 432.21 |
| P4 | 14.5 | – | – | 433.02 | 430.77 |
| P5 | 14.5 | + | + | 433.02 | 430.94 |
| P6 | 14.5 | – | – | 433.06 | 431.93 |
| P7 | 14.5 | – | – | 433.10 | 431.83 |
| P8 | 14.5 | – | – | 433.05 | 431.75 |
| P9 | 14.5 | – | – | 433.09 | 432.28 |
| P10 | 14.5 | – | – | 432.95 | 431.37 |
| P11 | 14.5 | – | – | 432.97 | 431.57 |
| P12 | 5.5 | – | – | 433.04 | 431.96 |
| P13 | 5.5 | – | – | 433.03 | 431.94 |
| P14 | 5.5 | – | – | 433.00 | 432.04 |
| P15 | 5.5 | – | – | [f] | [f] |
| P16 | 5.5 | + | + | 433.03 | 432.62 |
| P17 | 5.5 | + | + | 433.06 | 432.45 |
| P20 | 11.5 |  | – | 433.28 | 430.48 |
| P21 | 11.5 |  | – | 433.21 | 430.13 |
| P22 | 11.5 |  | – | 433.04 | 430.49 |
| P23 | 11.5 |  | – | 433.04 | 430.45 |
| P24 | 11.5 |  | – | 432.97 | 430.17 |
| P25 | 11.5 |  | – | 432.97 | 428.98 |
| P26 | 11.5 |  | – | 432.95 | 428.86 |
| P27 | 11.5 |  | – | 432.84 | 429.12 |
| P28 | 11.5 |  | – | 432.85 | 429.07 |

[a] Measured on June 17, 1996.
[b] All wells are screened the entire length in the ground water.
[c] Meters above sea level.
[d] Concrete wells were equipped with PVC piezometer tubes in May 1996.
[e] Not measured.
[f] Monitoring well is not accessible anymore.

### *Hydrogeological characteristics*

The field site (Figure 1) is located at 435 m above sea level in the *Berner Seeland*, one of the major gravel aquifers in the *Alpine Foreland Basin* (Biaggi et al. 1994). The aquifer consists of unconsolidated glaciofluvial outwash deposits. Drilling core material at the site consisted of 3–8 m of interbedded layers of poorly sorted silt, sand and gravel. The screened sections of most of the wells are in zones of gravel or sandy gravel. During the drilling of the boreholes P10, P13, P15, P25 and P26 at the north eastern part of the site, a zone of silt was found at the ground water table that extends into the saturated zone by up to 2 m and is underlain by sandy gravel. Only the screens of P25 and P26 reach this sandy gravel zone. The unconfined aquifer is underlain at 20–25 m depth by an aquitard, which consists of molasse sediments (Biaggi et al. 1994).

Hydraulic conductivities were determined by small single well pumping tests and were between $1.0 \times 10^{-4}$ and $9.3 \times 10^{-3}$ m s$^{-1}$ (Merkt & Stebler 1998). The porosity of the aquifer was assumed to correspond to that of a nearby similar geological formation, which was on average 0.19 (Jussel et al. 1994).

### *Hydrologic characteristics*

The ground water table at the site is generally 2–4 m below the surface and slopes in a north-easterly direction with a gradient of about 0.15 m per 100 m (Figure 1). From 1993 to 1996, the maximum fluctuation of the ground water table was 0.4 m. The temperature of the ground water changed seasonally between a minimum of 9.5 °C in March and a maximum of 11.5 °C in September. The main source of recharge to the *Berner Seeland* aquifer is precipitation as well as the river *Alte Aare* and the *Aare-Hagneck* channel, located 2.5 km and 15 km, from the site, respectively (Biaggi et al. 1994). Recharge from precipitation was estimated to be 0.44 m year$^{-1}$ (Biaggi et al. 1994). At the site recharge is lower because water collected on roofs and roads is discharged into the sewer system. The annual precipitation measured at the site was 1.08 m in 1995 and 0.58 m in 1996. During the natural gradient tracer experiment from August to December 1996, precipitation was only 0.19 m.

## Field and laboratory methods

### *Natural gradient tracer experiment*

On August 14, 1996, after geochemical sampling in June 1996, a natural gradient tracer experiment was started by the injection of KI, NaBr, and $H_3BO_3$ in the wells P2, PS3 and PS9, respectively. These tracers (all from Siegfried AG, Zofingen, Switzerland) were selected because they are considered to be conservative (Davis et al. 1980; Gelhar et al. 1992), not retarded by the residual oil and the background concentrations of these compounds in the aquifer of Studen are low ($<6$ $\mu$M). Three different injection wells were chosen to observe the transport characteristics at the site along the plume centerline and along its expected borders. Tracer solutions were prepared by mixing concentrated stock solutions of the tracers with water from a water supply well located about 1 km upgradient of the site in the same aquifer. The solutions were then injected into the saturated zone through the injection wells during a 24 to 26 hour period at the following rates: 4.6 l min$^{-1}$ in P2 (5 kg KI) and 9.3 l min$^{-1}$ in PS3 and PS9 (10 kg NaBr and 10 kg $H_3BO_3$, respectively). Large injection volumes were chosen to avoid the sinking of the tracer clouds due to the difference in density between the tracer solution and the ambient ground water (LeBlanc et al. 1991). Assuming a porosity of 0.19 and no mixing with ambient ground water, the initial volume of the aquifer occupied by the tracer solutions was about 74 m$^3$ at PS3 and PS9 and 37 m$^3$ at P2. Samples were taken at monitoring wells shown in Figures 2A and 2B before and immediately after completion of solute injection then every 3 to 4 days during the initial two weeks and every week during the following months. The breakthrough curves of the tracers in selected wells were interpolated and integrated. Mean flow velocities were calculated by dividing the distance from the injection well to the monitoring well by the time at which 50% of the tracer mass had passed this well (Matthess & Ubell 1983).

### *Ground water sampling techniques*

Ground water samples were collected using downhole submersible electrical pumps (Whale Superline 991, Munster Simms Engineering, Bangor, Northern Ireland) with teflon tubing (Maagtechnic, Dübendorf, Switzerland). At least two well volumes were removed before samples were taken.

Ground water samples for the analysis of dissolved monoaromatic hydrocarbons were collected in 40 ml

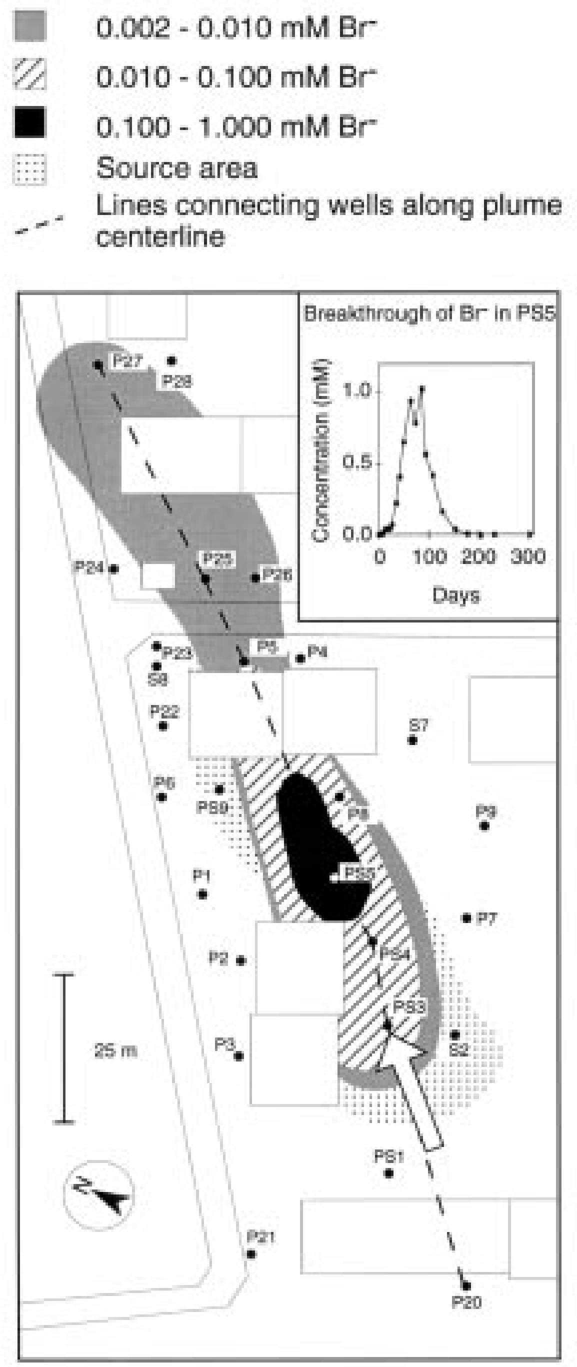

*Figure 2a.* Distribution of $Br^-$ 94 days after the injection into PS3 (arrow). Sampled monitoring wells shown only. In the insert, a typical example of a breakthrough curve is shown (at $Br^-$ PS5).

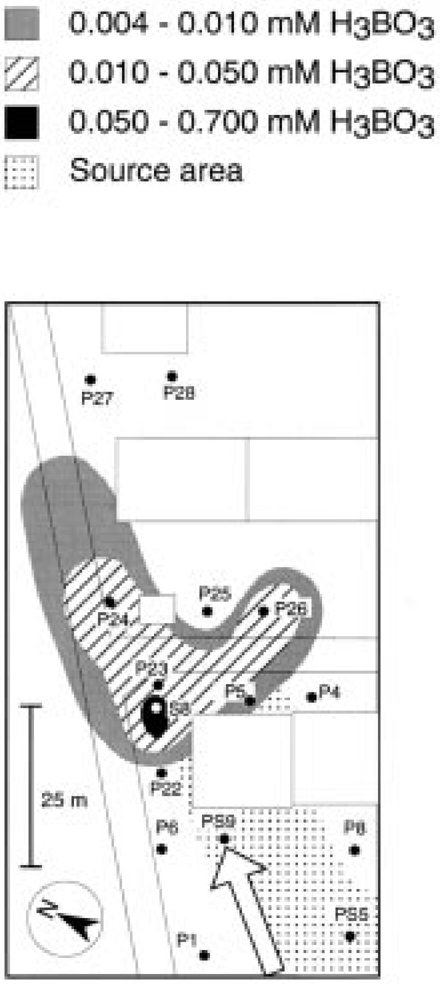

*Figure 2b.* Distribution of $H_3BO_3$ 94 days after the injection into PS9 (arrow). Sampled monitoring wells shown only.

glass vials, immediately acidified with 32% HCl to pH 2 and closed without head space with a Teflon-lined screw cap. Oxygen concentration, temperature, electrical conductivity, and pH were determined immediately at the site using the appropriate electrodes ($O_2$: Clark type electrode, WTW Oxi 96; temperature and conductivity: WTW LF 325; pH: WTW 95; all from WTW, Weilheim, Germany) fitted to a flow cell. Samples for analysis of dissolved species except for S(-II) were filtered in the field immediately after sampling using 0.22 $\mu$m polyvinylidenefluoride filters (Millipore, Bedford, USA). Samples for analysis of cations and dissolved metals were acidified with 0.1% distilled concentrated $HNO_3$; samples for S(-II) analysis were fixed using zinc acetate solution (APHA 1989). For alkalinity determinations and gas analysis, 117 ml serum bottles were filled and closed without head space using butyl rubber stoppers. Within 24 hours after sampling, a 20 ml head space of $N_2$ was introduced simultaneously with the removal of 20 ml of liquid, which was used for alkalinity determination. Gases were measured in the resulting head space after shaking followed by 12 hours of equilibration at 7 °C (Bossard et al. 1981). For stable carbon isotope analysis of the DIC, glass bottles (1000 ml) were filled with unfiltered ground water and closed without head space using rubber stoppers. Within 24 h after sampling, the DIC was precipitated as $BaCO_3$ by addition of 10 ml of a $CO_2$-free 2 M NaOH and 40 ml of a $CO_2$-free 1.2 M $BaCl_2$ solution. After more than 12 h of equilibration, the precipitate was filtered under a stream of $N_2$ and dried at 105 °C for 12 h.

### *Chemical analysis*

Total petroleum hydrocarbons were determined by infrared spectroscopy (APHA 1989). Samples for dissolved monoaromatic hydrocarbons were analyzed using a HP 5972A MS in selected ion monitoring mode interfaced to a HP 5890A Series II HRGC and a Tekmar LSC 2000 autosampler purge-and-trap system (Hewlett-Packard Ltd., USA and Tekmar, Cincinnati, USA). Monoaromatic hydrocarbon results reported are the average of two independent measurements.

Concentrations of $Cl^-$, $Br^-$, $NO_2^-$, $NO_3^-$, $SO_4^{2-}$, $PO_4^{3-}$ as well as $NH_4^+$, $Na^+$, $K^+$, $Ca^{2+}$ and $Mg^{2+}$ were determined with a Dionex DX-100 ion chromatograph (Dionex, Sunnyvale, USA). $H_3BO_3$ was determined spectrophotometrically using the method with azomethine-H as described in Fresenius et al. (1988). Dissolved Fe and Mn were quantified by atomic absorption spectroscopy in an air-acetylene flame (Varian SpectrAA 400, Varian Techtron, Springvale, Australia). It was assumed that the dissolved Fe and Mn consisted mainly of Fe(II) and Mn(II) respectively, because the solubility of Fe(III) is low at pH $< 6$ (Stumm & Morgan 1996). The terms Fe(II) and Mn(II) correspond to the sum of all dissolved species with the redox state +II. S(-II) was measured colorimetrically according to standard methods (APHA 1989) and represents the sum of $H_2S$, $HS^-$ and $S^{2-}$. Alkalinity was measured by potentiometric titration using Gran plots for graphical determination of the end point (Stumm & Morgan 1996). Charge balances were calculated to assure the accuracy of the analyses (Fritz 1994). The deviation between the sums of negative and positive charges was generally less than 10%. (Concentrations of $Cl^-$, $PO_4^{3-}$, $NH_4^+$, $Na^+$, and $K^+$ used in charge balances are not shown in Table 2).

The head space technique was used to quantify $CO_2$, $N_2O$ and $CH_4$ as described elsewhere (Bossard et al. 1981). The partial pressures of the gases were determined by gas chromatography (Carlo Erba Model 8000, Rodano, Italy) on a HayeSep D column using $N_2$ as carrier and a Carlo Erba thermal conductivity detector. Concentrations of dissolved gases were calculated according to Bossard et al. (1981) based on Henry's Law using the following Henry constants which are corrected for 7 °C: $CO_2$: 0.0594 mol $l^{-1}$ $atm^{-1}$ (Stumm & Morgan 1996); $N_2O$: 0.0449 mol $l^{-1}$ $atm^{-1}$ (Weiss & Price 1980); $CH_4$: 0.00206 mol $l^{-1}$ $atm^{-1}$ (Yamamoto et al. 1976); $C_2H_6$ 0.0032 mol $l^{-1}$ $atm^{-1}$ (Schwarzenbach et al. 1993). DIC concentrations were calculated from alkalinity and pH (Stumm & Morgan 1996).

### *Stable carbon isotope analysis*

All measured $^{13}C/^{12}C$ ratios are reported in the delta notation ($\delta^{13}C$) referenced to the VPDB standard (Coplen 1996). The $\delta^{13}C$ value is defined as:

$$\delta^{13}C = \frac{R_{\text{sample}} - R_{\text{standard}}}{R_{\text{standard}}} \cdot 1000 \qquad (1)$$

where $R_{\text{sample}}$ and $R_{\text{standard}}$ are the carbon isotope ratios in the sample and the standard, respectively. For stable carbon isotope analysis of the DIC, the dried $BaCO_3$ was converted to $CO_2$ at 90 °C in an automated acid bath preparation system using $H_3PO_4$ and then measured on a Fisons-Prism isotope-ratio mass spectrometer (Fisons, Middlewich, Cheshire, UK). For stable carbon isotope analysis of the carbonates in the aquifer material, a sample of mixed aquifer material from the drilling cores of P20 and P28 was ground, and the $\delta^{13}C$ was determined identically to the precipitated $BaCO_3$. The $\delta^{13}C$ of the PHC was measured using the free phase collected from S6 and P16. About 10 $\mu$l of the oil were combusted in an evacuated quartz tube at 950 °C during 3 h using 1 g CuO as an oxidant. The produced $CO_2$ was cryogenically purified on a vacuum line and analyzed. The analytical reproducibility of all $\delta^{13}C$ measurements was $<0.2‰$.

### *Stable carbon isotope balances*

The increase of DIC concentrations in wells of the contaminated site relative to uncontaminated wells upgradient was assessed using stable carbon isotope

*Table 2.* Chemical analysis of ground water samples collected June 17, 1996. Well names refer to Figure 1; T = Temperature; Alk = Alkalinity; DIC = Dissolved Inorganic Carbon

| Well | T °C | pH | Alk mM | DIC mM | $O_2$ mM | $NO_3^-$ mM | $SO_4^{2-}$ mM | S(II) mM | Fe(II) mM | Mn(II) mM | $CH_4$ mM | $Mg^{2+}$ mM | $Ca^{2+}$ mM | $\delta^{13}C$ ‰ |
|---|---|---|---|---|---|---|---|---|---|---|---|---|---|---|
| PS3 | 12.4 | 6.89 | 8.26 | 10.92 | 0.006 | 0.010 | 0.088 | 0.012 | 0.015 | 0.011 | 0.098 | 0.71 | 4.00 | −18.0 |
| PS4 | 12.5 | 6.73 | 9.48 | 13.88 | <0.003 | 0.010 | 0.021 | 0.003 | 0.197 | 0.055 | 0.684 | 0.89 | 4.92 | −16.1 |
| PS5 | 12.2 | 6.80 | 9.68 | 13.53 | 0.003 | <0.002 | 0.003 | 0.001 | 0.186 | 0.047 | 0.622 | 0.84 | 4.93 | −15.2 |
| S7 | 13.4 | 6.96 | 6.85 | 8.69 | 0.041 | 0.174 | 0.331 | [a] | <0.001 | <0.001 | 0.002 | 0.60 | 3.77 | −16.9 |
| S8 | 12.8 | 6.90 | 8.06 | 10.57 | 0.025 | 0.025 | 0.205 | [a] | <0.001 | 1.000 | <0.001 | 0.64 | 4.40 | [a] |
| PS9 | 11.6 | 6.90 | 7.57 | 9.99 | 0.003 | <0.002 | 0.398 | 0.010 | 0.010 | 0.007 | 0.006 | 0.61 | 3.96 | [a] |
| P1 | 11.3 | 6.96 | 6.08 | 7.78 | 0.022 | 0.008 | 0.335 | [a] | 0.077 | 0.003 | 0.010 | 0.51 | 3.19 | −16.0 |
| P2 | 12.3 | 6.94 | 6.04 | 7.77 | 0.009 | 0.008 | 0.484 | <0.001 | 0.001 | 0.006 | <0.001 | 0.69 | 3.12 | −15.5 |
| P3 | 12.4 | [a] | 5.52 | 7.56 | 0.025 | 0.010 | 0.516 | 0.003 | 0.003 | 0.001 | <0.001 | 0.59 | 3.24 | −13.6 |
| P4 | 11.4 | 7.15 | 6.70 | 7.90 | 0.016 | 0.159 | 0.198 | <0.001 | 0.000 | <0.001 | 0.001 | 0.70 | 3.39 | −15.6 |
| P5 | 13.2 | 7.06 | 7.36 | 8.92 | 0.003 | 0.101 | 0.190 | <0.001 | 0.053 | 0.011 | 0.218 | 0.71 | 3.61 | −16.0 |
| P6 | 13.4 | 7.03 | 5.71 | 7.01 | 0.019 | 0.082 | 0.405 | [a] | 0.007 | 0.004 | <0.001 | 0.52 | 3.05 | −14.9 |
| P7 | 12.0 | 6.96 | 6.98 | 8.90 | 0.025 | 0.198 | 0.289 | [a] | <0.001 | <0.001 | <0.001 | 0.70 | 3.52 | −16.0 |
| P8 | 11.7 | 6.99 | 7.29 | 9.18 | 0.006 | 0.064 | 0.233 | [a] | 0.018 | 0.021 | 0.058 | 0.72 | 3.61 | −17.0 |
| P9 | 11.6 | 6.97 | 6.67 | 8.48 | 0.066 | 0.146 | 0.211 | [a] | <0.001 | <0.001 | <0.001 | 0.67 | 3.47 | −15.7 |
| P20 | 11.8 | 7.14 | 6.43 | 7.61 | 0.018 | 0.258 | 0.326 | <0.001 | <0.001 | <0.001 | 0.005 | 0.73 | 3.41 | −14.4 |
| P21 | 11.0 | [a] | 6.77 | [a] | [a] | 0.055 | 0.270 | [a] | 0.016 | 0.010 | <0.001 | 0.71 | 3.44 | −14.8 |
| P22 | 11.3 | 7.14 | 6.38 | 7.55 | 0.025 | 0.129 | 0.331 | <0.001 | 0.001 | 0.001 | [a] | 0.69 | 3.30 | −15.0 |
| P23 | 11.6 | 7.12 | 6.41 | 7.63 | 0.004 | 0.110 | 0.377 | <0.001 | 0.001 | <0.001 | [a] | 0.70 | 3.42 | −15.8 |
| P24 | 12.6 | 7.11 | 6.92 | 8.27 | 0.008 | 0.081 | 0.277 | [a] | 0.001 | 0.001 | 0.002 | 0.70 | 3.43 | −16.3 |
| P25 | 11.5 | 7.14 | 6.86 | 8.12 | 0.009 | 0.162 | 0.264 | <0.001 | 0.001 | 0.003 | 0.025 | 0.75 | 3.60 | −15.5 |
| P26 | 11.0 | [a] | 6.62 | [a] | 0.003 | 0.185 | 0.292 | [a] | 0.001 | 0.002 | 0.003 | 0.71 | 3.41 | −14.6 |
| P27 | 11.1 | 7.15 | 6.77 | 7.99 | 0.010 | 0.242 | 0.336 | [a] | <0.001 | <0.001 | <0.001 | 0.73 | 3.47 | −15.2 |
| P28 | 13.3 | 7.14 | 6.86 | 8.06 | 0.012 | 0.180 | 0.295 | <0.001 | <0.001 | 0.001 | <0.001 | 0.71 | 3.46 | −15.3 |

[a] Not measured.

balances. As the ground water flowing through the source area becomes enriched in DIC, the $\delta^{13}C_{inc}$ is expected to change relative to the contributions of each of the $DIC_{inc}$ sources. This is expressed by the following two mass balance equations for $DIC_{meas}$ and $\delta^{13}C_{meas} * DIC_{meas}$ (Equations 2 and 3):

$$DIC_{meas} = DIC_{bg} + DIC_{inc} \tag{2}$$

$$\delta^{13}C_{meas} * DIC_{meas} = \delta^{13}C_{bg} * DIC_{bg} + \delta^{13}C_{inc} * DIC_{inc} \tag{3}$$

where $DIC_{meas}$ is the measured DIC concentration (mol $l^{-1}$), $DIC_{bg}$ is the measured DIC concentration upgradient (background P20) (mol $l^{-1}$), $DIC_{inc}$ is the DIC increase (mol $l^{-1}$), $\delta^{13}C_{meas}$ is the $\delta^{13}C$ of $DIC_{meas}$ (‰), $\delta^{13}C_{bg}$ is the $\delta^{13}C$ of $DIC_{bg}$ (‰), and $\delta^{13}C_{inc}$ is the $\delta^{13}C$ of $DIC_{inc}$ (unknown) (‰).

The mass balance (Equation 3) has the form of a linear equation. When the product of $\delta^{13}C_{meas} * DIC_{meas}$ is plotted versus $DIC_{inc}$, a straight line is obtained with a slope equal to the $\delta^{13}C_{inc}$ and an intercept of $\delta^{13}C_{bg} * DIC_{bg}$, according to Equation 3. Hence, the slope yields an overall average of the unknown isotopic ratio of the produced DIC in the contaminated zone.

## Results

### *Natural gradient tracer experiment*

Bromide tracer that was injected into PS3 was observed in PS4 immediately after the completion of the injection of the tracer solution. After 10 days it appeared in PS5, where concentrations increased until day 85 (Figure 2A, insert). As a selected example, the concentrations of bromide after 94 days are presented in Figure 2A. At that time, the center of mass of the bromide tracer had passed PS5 (Figure 2A, insert), and the front had already reached P27. The borate tracer injected in PS9 was first observed after 7 days simultaneously in P5, P23, P24 and P25. The concentration began to increase in S8 after 27 days. The concentration maximum of borate 94 days after the injection was found in S8, whereas it was no longer detected in P25 (Figure 2B). The iodide tracer injected in P2 disappeared completely from the injection well within

41 days. A breakthrough was observed only in P6 with first appearance after 107 days and a maximum concentration of 113 $\mu$M on day 126. In addition, iodide concentrations larger than the background concentration of 6 $\mu$M were observed occasionally in P1 (day 63 and 83) and in PS9 (day 26 and 34). Iodide was not observed in any other wells. Based upon these results we determined a general ground water flow direction of approximately 55° east.

The natural gradient tracer experiment was also used to calculate approximate residence times and mean flow velocities of the ground water and the dissolved species. The mean residence time of the bromide between PS3 and P5 was 125 days. The estimated residence time in the entire source area was approximately 165 days. Mean flow velocities determined by analysis of the breakthrough curves ranged from 0.3 m day$^{-1}$ (PS3 → PS4) to 0.8 m d$^{-1}$ (PS9 → P5).

### *PHC*

Dissolved monoaromatic hydrocarbons were found within the source area at a maximal total concentration of 123 $\mu$g l$^{-1}$ in PS5 (sum of all compounds shown in Figure 3). The corresponding maximal total petroleum hydrocarbon concentration measured was 1 mg l$^{-1}$ in PS5. No dissolved hydrocarbons were found outside of the source area. The concentrations of individual dissolved monoaromatic hydrocarbons measured in the source area along the plume centerline (see below) followed a similar trend each except for toluene, which was already depleted in P5 (Figure 3).

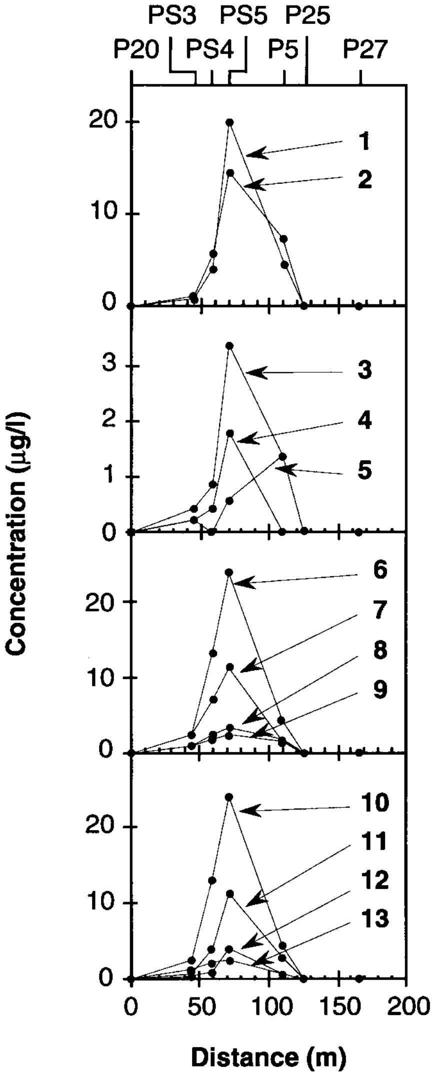

*Figure 3.* Concentrations of monoaromatic hydrocarbons in ground water samples of wells along the plume centerline, measured on July 16, 1997. (1) Sum of p- and m-xylene; (2) Ethylbenzene; (3) o-xylene; (4) toluene; (5) benzene; (6) sum of 3- and 4-ethylbenzene; (7) 2-ethylbenzene; (8) n-propylbenzene; (9) isopropylbenzene; (10) 1,2,4-trimethylbenzene; (11) 1,3,5-trimethylbenzene; (12) 1,2,3-trimethylbenzene; (13) sum of tetramethylbenzenes.

### *Temporal variability of ground water composition*

During the 41 month period in which detailed analysis of the chemical parameters in ground water at Studen were made (January 1995–May 1998), concentrations of important parameters remained fairly constant. As an example, we show $NO_3^-$ concentrations in 3 wells at the Studen site and in a well of drinking water facility located 1 km upgradient of the site (Figure 4). In all 4 wells the $NO_3^-$ concentrations remained constant, suggesting steady-state conditions. At the drinking water facility and in P20 the average $NO_3^-$ concentration and its standard deviation over the observed time period was 0.410 ± 0.021 mM and 0.278 ± 0.021 mM, respectively. The wells within (PS4) and just outside of the source area (P8) show consistently low $NO_3^-$ concentrations (average of 0.008 ± 0.008 mM and 0.065 ± 0.014 mM, respectively, Figure 4) indicating an increased but stable denitrification activity.

### *Ground water chemistry along the plume centerline*

Based on the distribution of the free phase, the transect P20 – PS3 – PS4 – PS5 – P5 – P25 – P27 was chosen as a streamline representing the plume centerline (Figure 2A). Of the seven selected wells, one is located upgradient of the source area (P20), four are

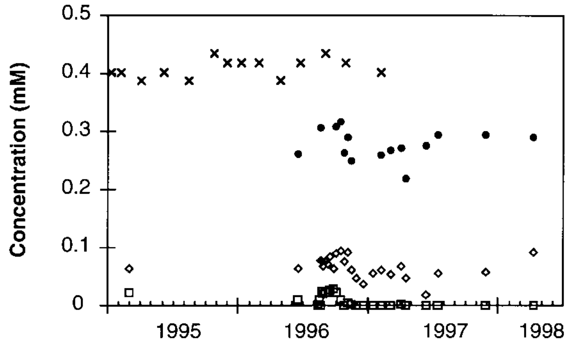

*Figure 4.* $NO_3^-$ concentrations in selected wells from January 1995 to May 1998. ×: Drinking water facility 1 km upstream of the site; ●: P20; ◊: P8; □: PS5.

within the source area (PS3, PS4, PS5, P5) and two are downgradient of the source area (P25 and P27).

All values of chemical parameters measured on June 17, 1996, which represents a typical profile encountered at the Studen site, are reported in Table 2. Values in wells, which represent the plume centerline are plotted against the distance of the respective wells from P20 (Figure 5). Oxidants ($O_2$, $NO_3^-$, $SO_4^{2-}$) were consumed within the source area and reached background concentrations again downgradient (Figure 5). In the monitoring wells within the source area, dissolved Fe(II) and Mn(II) were detected. Concentrations of S(-II) were above detection limit only in PS3 (0.012 mM) and PS4 (0.003 mM). $CH_4$ was found in PS3, PS4, PS5 and P25 (Figure 5). The $N_2O$ concentration was below 0.005 mM; $NO_2^-$ and $PO_4^{3-}$ concentrations were below the detection limit of 0.002 mM in all measured monitoring wells. Alkalinity, DIC and $Ca^{2+}$ were elevated within the source area. The $Mg^{2+}$ concentration showed no changes over the length of the plume centerline. In all wells along the plume centerline, the $\delta^{13}C$ of the DIC was found to be more negative than upgradient in P20 (Figure 5). The most negative $\delta^{13}C$ was measured in PS3 at the upgradient border of the source area.

### *Stable carbon isotope balances*

As shown in Table 3, different DIC sources have distinct isotopic ratios. Non-methanogenic PHC mineralization yields DIC with a negative $\delta^{13}C$ (−27.8‰; measured $\delta^{13}C$ of the Studen oil), carbonate dissolution yields DIC with a $\delta^{13}C$ of around zero (−1.1‰, measured in aquifer material from Studen), and methanogenesis yields DIC with a positive $\delta^{13}C$ (+38‰, see Table 3).

From all the wells printed in bold in Figure 1, the product of $\delta^{13}C_{meas} * DIC_{meas}$ is plotted versus $DIC_{inc}$ in Figure 6 according to Equation 3. The slopes of possible different sources of DIC are shown in the insert of Figure 6 as vector A (non-methanogenic PHC mineralization; slope = −27.8‰), vector B (carbonate dissolution; slope = −1.1‰, and vector C (methanogenic PHC mineralization; slope = +38‰).

A least square linear regression analysis of data measured on June 17, 1996 from monitoring wells labelled in bold in Figure 1 was performed. Data from wells with methane concentrations <0.1 mM yield a slope of −24.4‰ ($R^2$ = 0.96). Wells having methane concentrations >0.1 mM (PS4 and PS5) show, as expected, a deviation from vector A towards more positive values (Figure 6). In wells containing no or little methane, all $DIC_{inc}$ can be attributed either to non-methanogenic hydrocarbon mineralization (fraction $f_h$) or carbonate dissolution (fraction $f_c$). Based upon the distinct $\delta^{13}C$ values of these processes Equation 4 is established.

$$f_h * (-27.8‰) + f_c * (-1.1‰) = -24.4‰ \qquad (4)$$

Considering the fact that $f_h + f_c = 1$, Equation 4 yields $f_h$ = 0.88, signifying that in the average over all wells, 88% of the DIC increase originates from non-methanogenic PHC mineralization and 12% from carbonate dissolution.

### *Equilibria of geochemical processes*

Saturation calculations for minerals that can potentially undergo precipitation or dissolution were performed as described in Hunkeler (1999) in order to identify geochemical reactions which might influence the concentrations of DIC, Fe(II), Mn(II), $Ca^{2+}$ and S(-II). The ground water at the Studen site is saturated or slightly supersaturated with respect to $CaCO_3$ (calcite). No distinct differences were observed in the calcite saturation between monitoring wells in the source area to wells outside of the source area. All monitoring wells were undersaturated with respect to $MnCO_3$ (rhodocrosite). PS4, PS5 and P5 were the only wells that were supersaturated with respect to $FeCO_3$ (siderite).

*Table 3.* Stoichiometric equations of selected processes involved in hydrocarbon mineralization[a]

| Process | Contribution to DIC[b] | Contribution to alkalinity[b] | $\delta^{13}C$ of $DIC_{inc}$ (‰) |
|---|---|---|---|
| *Microbial hydrocarbon mineralization*[c] | | | |
| $0.68\langle CH_{1.85}\rangle + \mathbf{O_2} \rightarrow 0.68CO_2 + 0.63H_2O$ | + 0.68 | 0 | −27.8[d] |
| $0.85\langle CH_{1.85}\rangle + \mathbf{NO_3^-} + H^+ \rightarrow 0.85CO_2 + 0.5N_2 + 1.29H_2O$ | +0.85 | +1 | −27.8[d] |
| $0.34\langle CH_{1.85}\rangle + MnO_2(s) + 2H^+ \rightarrow 0.34CO_2 + \mathbf{Mn^{2+}} + 1.31H_2O$ | + 0.34 | +2 | −27.8[d] |
| $0.17\langle CH_{1.85}\rangle + FeOOH(s) + 2H^+ \rightarrow 0.17CO_2 + \mathbf{Fe^{2+}} + 1.66H_2O$ | +0.17 | +2 | −27.8[d] |
| $1.37\langle CH_{1.85}\rangle + \mathbf{SO_4^{2-}} + 2H^+ \rightarrow 1.37CO_2 + H_2S + 1.26H_2O$ | +1.37 | +2 | −27.8[d] |
| $1.37\langle CH_{1.85}\rangle + 0.74H_2O \rightarrow 0.37CO_2 + \mathbf{CH_4}$ | +0.37 | 0 | +38[e] |
| *Geochemical processes* | | | |
| $CaCO_3(s) + 2H^+ \leftrightarrow CO_2 + \mathbf{Ca^{2+}} + H_2O$ | +1 | +2 | −1.1[f] |
| $CO_2 + Fe^{2+} + H_2O \rightarrow FeCO_3(s) + 2H^+$ | −1 | −2 | [g] |
| $Fe^{2+} + H_2S \rightarrow FeS(s) + 2H^+$ | 0 | −2 | |

[a] All species are given in the form in which they exist at the reference point of the alkalinity titration (pH=4.3). Thus the number of protons that are produced or consumed corresponds to alkalinity consumption or production. The species printed bold were used to quantify the processes.

[b] Moles per mole stoichiometric turnover of species printed bold.

[c] It was assumed that hydrocarbons in heating oils have an average H/C ratio of 1.85 (denoted as $\langle CH_{1.85}\rangle$). Biomass formation is assumed to be negligible.

[d] The $\delta^{13}C$ of DIC produced by non-methanogenic microbial hydrocarbon mineralization assumed to be not subject to any fractionation (Hunkeler 1997; Aggarwal et al. 1997).

[e] Methanogenic PHC mineralization is reported to enrich $\delta^{13}C$ of DIC up to +38‰ (Grossman, 1997).

[f] Measured $\delta^{13}C$ of carbonate in a mixed sample of the aquifer material from P20 and P28.

[g] Depends on $\delta^{13}C$ of the precipitating DIC and fractionation factor between the DIC and the $FeCO_3$ (Deines et al. 1974; Carothers et al. 1988).

## Discussion

### *Natural gradient tracer experiment*

The determination of the flow direction based on hydraulic heads at sites with small gradients and a free phase of PHC in the monitoring wells is subject to considerable uncertainty (Bedient et al. 1994). Therefore, a tracer experiment using conservative tracers in three different injection wells was performed to get a better understanding of transport within, and downgradient of the source area. A general flow direction at this site of approximately 55° east was obtained from the bromide and borate tracer injections. The trajectory of the center of the iodide cloud could not be detected, probably because it travelled to the northeast of all wells. This flow path would be consistent with predictions based on hydraulic heads (Figure 1).

### *Influence of physical processes on concentration profiles*

The concentrations of measured species in the ground water may be influenced by mixing with pristine ground water, which can occur by two ways: either by vertical and lateral mixing in the aquifer (dispersive mixing) or during sampling within the monitoring well. When interpreting the chemical data along the plume, one has to be aware that they are significantly influenced by the screen lengths and the vertical extension of the plume. Incorrect assessment of vertical concentration profiles can lead to false interpretation of plume lengths, plume directions and even source zone location (Martin-Hayden & Robbins 1997).

At our site, most monitoring wells were drilled by the cantonal authorities to allow an initial survey of the extension of the contaminated zone and reach to different depths (Table 1). Wells PS3, PS4 and PS5 had a screened length of less than 0.7 m below the ground water table, whereas wells P5, P20, P25 and P27 had a screened length of 2.08, 2.80, 3.99 and 3.72 m respectively below the ground water table. Thus the chemical data presented in Figures 3 and 5 may partially reflect the screen length but these data give a qualitative insight into the respective processes.

### *Dissolved monoaromatic hydrocarbons*

We focused our attention on monoaromatic hydrocarbons because of their toxicity and their higher water

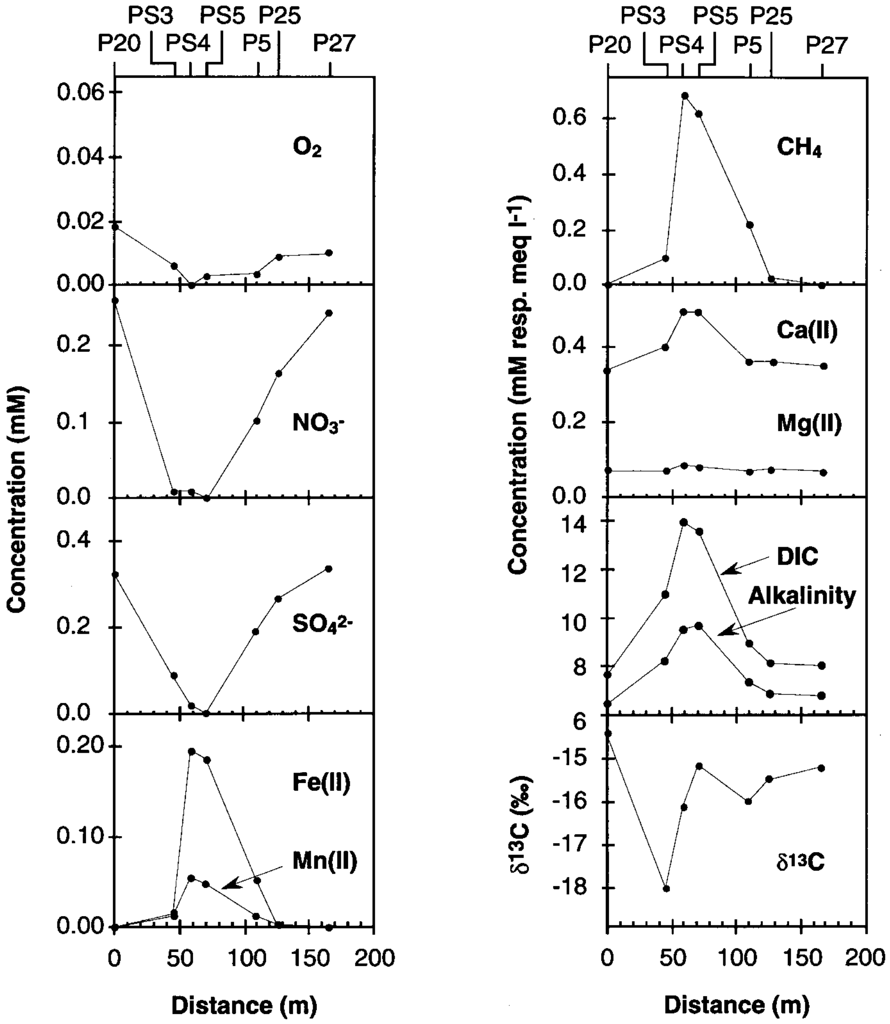

*Figure 5.* Ground water chemistry along the plume centerline on June 17, 1996.

solubilities compared to other hydrocarbons present in heating oil (Eganhouse et al. 1996). Dissolved monoaromatic hydrocarbons are therefore the oil constituents that most likely form a plume. The elevated concentrations along the plume centerline show that monoaromatic hydrocarbons dissolve from the residual PHC pool into the water phase within the source area. However, contrary to the non-reactive tracers, monoaromatic hydrocarbons are not found in monitoring wells downgradient of the source area (P23, P25, P27). In fact, a decrease of hydrocarbon concentration within the source area can be observed from PS5 to P5 (Figure 3). It must be noted that disappearance of hydrocarbons alone is not a proof of intrinsic bioremediation (MacDonald & Rittmann 1993). Other natural attenuation effects such as dilution, sorption, or preferential flow paths can lead to a diminishing hydrocarbon concentration. At Studen, the disappearance of hydrocarbons is probably due to a number of processes including dilution, sorption, and biodegradation. Eganhouse et al. (1996) showed selective biodegradation of single monoaromatic compounds at another site. Whether the same is also true for the Studen site remains open and is subject to further studies.

### *Microbiological and geochemical processes*

The monitoring in the source zone showed decreased levels of oxidants and increased levels of reduced species, DIC, and alkalinity within the source area with respect to the background concentrations. This in-

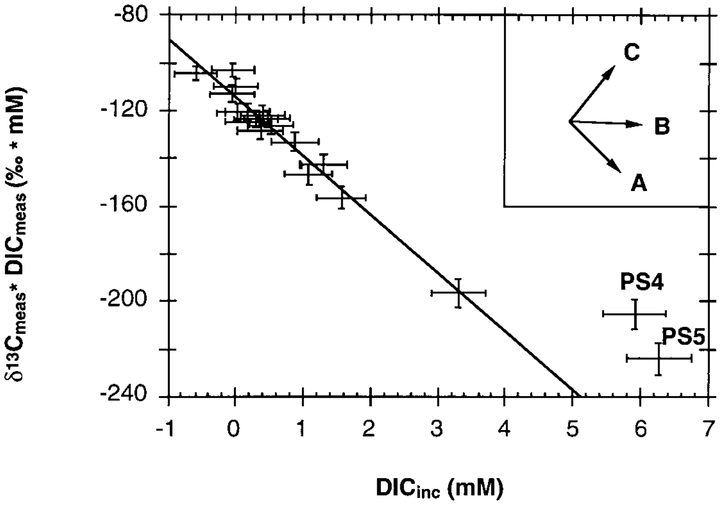

*Figure 6.* $\mathrm{DIC_{meas}} * \delta^{13}\mathrm{C_{meas}}$ plotted versus $\mathrm{DIC_{inc}}$ for wells whose names are in bold characters in Figure 1 measured on June 17, 1996. Vectors indicating the source of $\mathrm{DIC_{inc}}$: A – $\mathrm{DIC_{inc}}$ produced by non-methanogenic PHC mineralization, B – $\mathrm{DIC_{inc}}$ produced by carbonate dissolution, C – $\mathrm{DIC_{inc}}$ produced by methanogenic PHC mineralization.

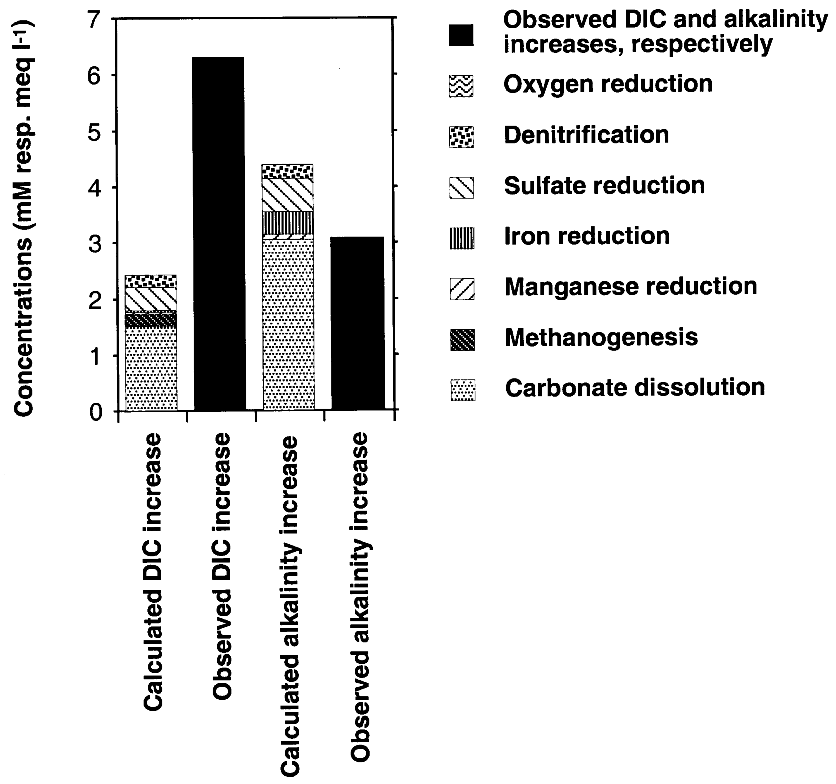

*Figure 7.* DIC and alkalinity balances along the flowpath P20–PS4.

dicates increased microbial activity within the source area. Changes in concentrations of species measured in P5, P25, and P27 towards background concentrations (Figure 5) may be partly explained by the mixing of plume water with pristine ground water during sampling, as discussed above.

Based on the observed concentrations of oxidants and reduced species at the Studen site and saturation calculations, we propose that the microbial and geochemical processes shown in Table 3 are the most significant ones in our aquifer. We are fully aware that other processes also take place in the aquifer; however, the chosen processes seem to be the dominant, quantifiable processes. Similar processes have been shown to be relevant in ground water biogeochemistry in laboratory studies (Hess et al. 1996; Hunkeler et al. 1998) and other field sites (Herczeg et al. 1991; Hunkeler 1997). Production of DIC from naturally occuring DOC is excluded for quantitative reasons, since the observed increases of up to 7 mM DIC is far higher than the DOC concentrations observed in the aquifer (0–0.22 mM, Kozel 1992). The ground water that enters the site is saturated with respect to $CaCO_3$ (calcite) but undersaturated with respect to $FeCO_3$ (siderite), $MnCO_3$ (rhodocrosite) and FeS (amorphous iron sulfide). The observed increase in dissolved $Ca^{2+}$ within the source area is due to the dissolution of $CaCO_3$. The large formation of $CO_2$ within the source area causes significantly lower pH values in these monitoring wells (Table 2). The pH drop leads to the dissolution of calcite to reach saturated conditions again.

### *Stable carbon isotope balances*

Stable carbon isotope ratios in inorganic carbon have been used previously to verify non-methanogenic petroleum hydrocarbon mineralization by showing that the inorganic carbon has the same isotopic ratio ($-27‰$ to $-30‰$) as the PHC (Van de Velde et al. 1995; Aggarwal et al. 1997). However, at sites where methanogenesis occurs, the $\delta^{13}C$ in DIC were reported to range from around $-30‰$ up to $+11.9‰$ (Landmeyer et al. 1996; Conrad et al. 1997), adding serious difficulties to the proving of PHC mineralization. Conrad and co-workers (1997) suggested the use of $^{14}C$ to correct for this, however, $^{14}C$-analyses are costly.

We developed a graphical method (Figure 6) based on $\delta^{13}C$ in DIC only, which allows one to display the data from different non-methanogenic and methanogenic monitoring wells from a heterogeneous field site. Samples from wells with methane concentrations $>0.6$ mM (PS4 and PS5) deviate clearly from the trend of all other wells. The wells with $<0.1$ mM methane are all lying on a straight line having the slope of $-24.4‰$ in Figure 6 although their DIC concentrations may have been influenced by mixing processes due to the different screen lenghts of the wells. The mixing of a water sample containing high DIC concentrations with a pristine water sample containing background DIC concentrations (e.g. from deep aquifer strata) has the effect that the data point in Figure 6 moves up along the slope towards the intercept. Thus, mixing with pristine ground water during sampling does not affect the slope of Equation 3 and the conclusions drawn from it. However, it has to be stated that the graphical method yields only a defined slope in an aquifer where the relative contributions of mineralization and carbonate dissolution are constant. Also, there is concern that in very shallow monitoring wells, the volatilization of $CO_2$ might add some uncertainty, since lighter isotopes tend to volatilize more easily (Stumm & Morgan, 1996).

The assessment of the slope yielded in Figure 6 allowed to conclude that PHC mineralization is the predominant process of DIC production in this aquifer under the assumption that natural organic matter is not considered as a source of DIC. Similar contributions of PHC mineralization and carbonate dissolution were reported by Revesz et al. (1995) at a field site contaminated with crude oil. However, in aquifers where larger quantities of particulate or dissolved natural organic matter are oxidised to DIC, the assessment of PHC mineralization has to include also $^{14}C$ data, since the $\delta^{13}C$ in natural organics and in PHC are similar (Baedecker et al. 1993; Conrad et al. 1997).

### *DIC and alkalinity balances*

These balances are based on a comparison of calculated increases due to stoichiometric considerations with observed increases (Hunkeler 1997). The calculated DIC increase was determined using the measured consumption of oxidants and production of reduced species and $Ca^{2+}$ and the stoichiometric equations shown in Table 3. The observed DIC increase is the measured difference in DIC concentration. The calculated alkalinity increase and observed alkalinity increase accompanying microbial hydrocarbon mineralization were determined analogously. In order to quantify the proposed processes, the following assumptions had to be made: i) steady-state conditions were established, ii) the oxidants were used to mineralize hydrocarbons exclusively and iii) no gas exchange between the unsaturated and the saturated zone occurred. The biases of the first and second assumptions are considered to be only minor: the chemical concentrations show no trends towards increased or decreased concentrations with only minor variations (Figure 4) and the ground water in the vicinity of the site has a low content in dissolved organic matter (DOC $< 0.22$ mM, Kozel 1992). However, the extent of gas exchange between the unsaturated and the saturated zone is presently unknown.

DIC and alkalinity balances were established for the flow paths between P20 and the monitoring wells in the plume centerline. In shallow wells (PS3, PS4 and PS5) mixing with pristine ground water during sampling can be neglected and therefore the flow path from P20 to PS4 was selected to illustrate DIC and alkalinity balances (Figure 7). The calculated DIC increase based on the stoichiometric factors (Table 3) and the measured species in ground water was only about one third of the observed DIC increase (Figure 7). On the other hand, the observed alkalinity increase is smaller than the calculated alkalinity increase (Figure 7).

Considering the balances, a number of processes listed in Table 3 have to be discussed in detail. Fe(III) reduction is underestimated as the microbially produced Fe(II) reacts, e.g. with S(-II) or $CO_3^{2-}$ and precipitates as FeS or $FeCO_3$. The Fe(II) concentration found in ground water is therefore likely to be lower than the actual produced Fe(II) concentration. The reduction of 1 mol Fe(III) produces 0.17 mol DIC and 2 mol alkalinity, whereas the precipitation of Fe(II) consumes 1 mol DIC and 2 mol alkalinity (Table 3). The fate of the sulfur of $SO_4^{2-}$ after its reduction to $H_2S$ is unknown. Possible reactions are precipitation with metals, reoxidation, or transport to the unsaturated zone. The turnover of $SO_4^{2-}$ is therefore underestimated when only the concentrations in the ground water are compared. The reduction of $SO_4^{2-}$ contributes to the alkalinity balance and is the major contributor to the DIC balance per mol turnover (Table 3). However, precipitation of $H_2S$ affects only the alkalinity balance. The gas exchange might also play a significant role. Aerobic hydrocarbon mineralization and methanogenesis may be underestimated because the amounts of $CH_4$ escaping and $O_2$ entering the system through the unsaturated zone are unknown. Both processes would lead to an increase in the calculated DIC without affecting alkalinity (Table 3) and were observed in an aquifer contaminated by crude oil (Revesz et al. 1995).

We assume that all of the above mentioned processes are involved in the production of the unaccounted DIC. Similar discrepancies in calculated production and measured increase of DIC and alkalinity were observed in all monitoring wells along the plume centerline, as well as at other field sites (Bennett et al. 1993; Hunkeler 1997). In order to further improve the mass balance to be used as a reliable assessment tool, the gaseous and solid phases must be considered as well.

## Conclusions

Despite the fact that the site in Studen contains inherent obstacles to the establishment of a quantitative assessment of intrinsic bioremediation, we were able to gather strong evidence for microbial PHC mineralization by the measurement of different independent lines of evidence. The natural gradient tracer test gave solid information about the direction and the velocity of the ground water transport at the site. Hydrocarbon analysis showed the presence of dissolved monoaromatic hydrocarbons in the source area, but concentrations in wells situated downgradient of the source area were below detection limit. However, absolute concentrations of dissolved species have to be interpreted with great care since they tend to depend on the vertical extension of the plume and on the screen length of the monitoring wells (Martin-Hayden & Robbins 1997). The monitoring of hydrocarbons, oxidants, reduced species and DIC in the ground water along and perpendicular to the plume centerline reflected microbiological activity and geochemical reactions in the aquifer. Oxidants were decreased and reduced species, $Ca^{2+}$, alkalinity, and DIC were increased within the source area. But DIC and alkalinity balances in shallow monitoring wells, which were not affected by dilution, revealed that not all processes had been correctly accounted for. This disagreement indicates that the quantification of PHC mineralization is underestimated when only concentrations in the ground water are used for the calculation of the balances. The new graphical method to interpret stable carbon isotope ratios of the DIC was used instead to prove the microbial mineralization of PHC. It was shown that 88% of the produced DIC originates from non-methanogenic PHC mineralization at this site. These results indicate enhanced biological activity in the source area and its borders. The conclusion drawn from $\delta^{13}C$ data has the advantage of not being affected by the differences in the screen lengths of the wells. In summary, the presented data show that a heating oil-contaminated aquifer with a low $O_2$ background concentration can potentially be treated by intrinsic bioremediation. Further studies are being undertaken to better understand the vertical profile of dissolved species and to quantify additional processes such as precipitation and dissolution reactions.

## Acknowledgment

The authors thank J.P. Clément and P. Wersin (Amt für Gewässerschutz und Abfallwirtschaft, Kanton BE) for their cooperation at the field site, and J. McKenzie and S. Bernasconi (ETH) for providing the facilities for isotope analysis. A special thanks to Chr. Gruber (BMG Engineering AG), E. Höhn (EAWAG), T. Hug, M. Gabriel, F. Stauffer, and W. Kinzelbach (ETH) for assistance with the natural gradient tracer experiment. The analysis of hydrocarbons by M. Schluep (BMG Engineering AG) is gratefully acknowledged. The paper benefited by the corrections by G.T. Townsend and M.H. Schroth (ETH). The work was supported by the Swiss National Science Foundation (Priority Programme Environment).

## References

Aggarwal PK, Fuller ME, Gurgas MM, Manning JF & Dillon MA (1997) Use of stable oxygen and carbon isotope analyses for monitoring the pathways and rates of intrinsic and enhanced in situ biodegradation. Environmental Science and Technology 31: 590–596

APHA (1989) Standard methods for the examination of water and wastewater. American Public Health Association, Clesceri LS, Greenberg AE & Trussell RR (Eds), Washington DC

ASTM (1995) Standard guide for risk-based corrective action applied at petroleum release sites. American Society for Testing and Materials, West Conshohocken

Atlas RM & Bartha R (1992) Hydrocarbon biodegradation and oil spill bioremediation. Advances in Microbiological Ecology 12: 287–338

Baedecker MJ, Cozzarelli IM, Eganhouse RP, Siegel DI & Bennett PC (1993) Crude oil in a shallow sand and gravel aquifer – III Biogeochemical reactions and mass balance modeling in anoxic groundwater. Applied Geochemistry 8: 569–586

Bedient PH, Rifai HS & Newell CJ (1994) Ground water contamination: transport and remediation. Prentice Hall, Englewood Cliffs, NJ

Bennett PC, Siegel DE, Baedecker MJ & Hult MF (1993) Crude oil in a shallow gravel aquifer – I. Hydrogeology and inorganic geochemistry. Applied Geochemistry 8: 529–549

Biaggi D, Bossart P, Kuhlmann U & Muchenberger F (1994) Modellierung der Strömung und der Nitratausbreitung im Berner Seeland, Schweiz. Eclogae Geologicac Helvetiae 87: 429–438

Borden RC, Gomez CA & Becker MT (1995) Geochemical indicators of intrinsic bioremediation. Ground Water 33:180–189

Bossard P, Joller T & Szabo E (1981) Die quantitative Erfassung von Methan im Seewasser. Schweizerische Zeitschrift für Hydrologie 43: 200–211

Boulding JR (1995) Practical handbook of soil, vadose zone, and ground-water contamination: Assessment, prevention, and remediation. Lewis Publishers, Boca Raton

Boutton TW (1991) Stable carbon isotope ratios of natural materials: II. Atmospheric, terrestrial, marine, and freshwater environments. In: Coleman DC & Fry B (Eds) Carbon isotope techniques (pp 173–185). Academic Press, San Diego

Carothers WW, Adami LH & Rosenbauer RJ (1988) Experimental oxygen isotope fractionation between siderite-water and phosphoric acid liberated $CO_2$-siderite. Geochimica et Cosmochimica Acta 52: 2445–2450

Carothers WW & Kharaka K (1980) Stable carbon isotopes of $HCO_3^-$ in oil-field waters – implications for the origin of $CO_2$. Geochimica et Cosmochimica Acta 44: 323–332

Conrad ME, Daley PF, Fischer ML, Buchanan BB, Leighton T & Kashgarian M (1997) Combined $^{14}C$ and $\delta^{13}C$ monitoring of in situ biodegradation of petroleum hydrocarbons. Environmental Science and Technology 31: 1463–1469

Coplen TB (1996) New guideline for reporting stable hydrogen, carbon, and oxygen isotope-ratio data. Geochimica et Cosmochimica Acta 60: 3359–3360

Davis JW, Klier NJ & Carpenter CL (1994) Natural biological attenuation of benzene in ground water beneath a manufacturing facility. Ground Water 32: 215–226

Davis SN, Thompson GM, Bemtley HW & Stiles G (1980) Ground water tracers – a short review. Ground Water 18: 14–23

Deines P & Langmuir D (1974) Stable carbon isotope ratios and the existence of a gas phase in the evolution of carbonate ground water. Geochimica et Cosmochimica Acta 38: 1147–1164

Eganhouse RP, Baedecker MJ, Cozzarelli IM, Aiken GR, Thorn KA & Dorsey TF (1993) Crude oil in a shallow sand and gravel aquifer – II Organic geochemistry. Applied Geochemistry 8: 551–567

Eaganhouse RP, Dorsey TF, Phinney CS & Westcott AM (1996) Processes affecting the fate of monoaromatic hydrocarbons in an aquifer contaminated by crude oil. Environmental Science and Technology 30: 3304–3312

Fresenius W, Quentin KE & Schneider W (1988) Water analysis. Springer, New York

Fritz SJ (1994) A survey of charge-balance errors on published analyses of potable ground and surface waters. Ground Water 32: 539–546

Gelhar LW, Welty C & Rehfeldt KR (1992) A critical review of data on field-scale dispersion in aquifers. Water Resources Research 28: 1955–1974

Grossman, EL (1997) Stable carbon isotopes as indicators of microbial activity in aquifers. In: Hurst CJ (Ed) Manual of environmental microbiology, (pp 565–576), American Society for Microbiology, Washington DC

Herczeg AL, Torgersen T, Chivas AR & Habermehl MA (1991) Geochemistry of ground waters from the Great Artesian Basin. Australia Journal of Hydrology 126: 225–246

Hess A, Höhener P, Hunkeler D & Zeyer J (1996) Bioremediation of a diesel fuel contaminated aquifer: Simulation studies in laboratory aquifer columns. Journal of Contaminant Hydrology 23: 329–345

Holliger C & Zehnder AJB (1996) Anaerobic biodegradation of hydrocarbons. Current Opinion in Biotechnology 7: 326–330

Hunkeler D (1997) Assessment and quantification of bioremediation in anaerobic aquifers. Ph.D. Thesis Nr. 12268 ETH Zürich

Hunkeler D, Höhener, P, Bernasconi S & Zeyer J (1999) Engineered in situ bioremediation of a petroleum hydrocarbon-contaminated aquifer: Assessment of mineralization based on alkalinity, inorganic carbon and stable carbon isotope balances. Journal of Contaminant Hydrology: 37: 201–223

Hunkeler D, Jörger D, Haberli K, Höhener P & Zeyer J (1998) Petroleum hydrocarbon mineralization in anaerobic laboratory aquifer columns. Journal of Contaminant Hydrology 32: 41–61

Jussel P, Stauffer F & Dracos T (1994) Transport modeling in heterogeneous aquifers 1. Statistical description and numerical generation of gravel deposits. Water Resources Research 30: 1803–1817

Kozel R (1992) The detection of organic pollutants, i.e. pesticides, in near-surface porous aquifers (in German). Ph.D. Thesis, University of Neuchâtel, Switzerland

Krumholz LR, Caldwell ME & Suflita JM (1996) Biodegradation of BTEX hydrocarbon compounds under anaerobic conditions. In: Crawford RL & Crawford DL (Ed) Bioremediation Principles and Applications (pp 61–99). Cambridge University Press, Cambridge

Landmeyer JE, Vroblesky DA & Chapelle FH (1996) Stable carbon isotope evidence of biodegradation zonation in a shallow jet-fuel contaminated aquifer. Environmental Science and Technology 30: 1120–1128

LeBlanc DR, Garabedian SP, Hess KM, Gelhar LW, Quadri RD, Stollenwerk KG & Wood WW (1991) Large-scale natural gradient tracer test in sand and gravel, Cape Cod, Massachusetts 1. Experimental design and observed tracer movement. Water Resources Research 27: 895–910

MacDonald JA & Rittmann BE (1993) Performance standards for in situ bioremediation. Environmental Science and Technology 27: 1974–1979

Madsen EL, Sinclair JL & Ghiorse WC (1991) In situ biodegradation: Microbiological patterns in a contaminated aquifer. Science 252: 830–833

Martin-Hayden JM & Robbins GA (1997) Plume distortion and apparent attenuation due to concentration averaging in monitoring wells. Ground Water 35: 339–346

Matthess G & Ubell K (1983) Allgemeine Hydrogeologie – Grundwasserhaushalt. Lehrbuch der Hydrogeologie. Gebrüder Borntraeger, Berlin

McAllister PM & Chiang CY (1994) A practical approach to evaluating natural attenuation of contaminants in ground water. Ground Water Monitoring and Remediation 14: 161–173

Merkt C & Stebler T (1998) Grundwassermodell für die Sanierung eines heizölkontaminierten Grundwasserleiters in der Gemeinde Studen (BE). Diplomathesis, Institute of Terrestrial Ecology ETH Zürich

Revesz K, Coplen TB, Baedecker MJ & Glynn PD (1995) Methane production and consumption monitored by stable H and C isotope ratios at a crude oil spill site, Bemidji, Minnesota. Applied Geochemistry 10: 505–516

Rifai HS, Borden RC, Wilson JT & Ward CH (1995) Intrinsic bioattenuation for subsurface restoration. In: Hinchee RE, Wilson JT & Downey DC (Eds) Intrinsic bioremediation, Vol 1 (pp 1–31). Battelle Press, Columbus

Schwarzenbach RP, Gschwend PM & Imboden DM (1993) Environmental organic chemistry. John Wiley & Sons, New York

Stumm W & Morgan JJ (1996) Aquatic chemistry, 3rd ed. John Wiley and Sons, New York

U.S. National Research Council (1993) *In situ* bioremediation – when does it work? National Academy Press, Washington DC

Van de Velde KD, Marley MC, Studer J & Wagner DM (1995) Stable carbon isotope analysis to verify bioremediation and bioattenuation. In: Hinchee RE, Douglas GS & Ong SK (Eds) Monitoring and verification of bioremediation, Vol 5 (pp 241–257). Battelie Press, Columbus, Ohio

Vroblesky DA & Chapelle FH (1994) Temporal and spatial changes of terminal electron-accepting processes in a petroleum hydrocarbon-contaminated aquifer and the significance for contaminant biodegradation. Water Resources Research 30: 1561–1570

Weiss RF & Price BA (1980) Nitrous oxide solubility in water and seawater. Marine Chemistry 8: 347–359

Yamamoto S, Alcauskas JB & Crozier TE (1976) Solubility of methane in distilled water and seawater. Journal of Chemical and Engineering Data 21: 78–80